a minimum for the SiS compounds. This trend will probably be more pronounced in similar Ge- and Sn-containing species. Hence it follows that a strong triple bond is found only in CO.

Ahlrichs showed a direct connection between SENs and bond energy.[17] This connection is also true for the molecules under discussion if one compares only the carbon- or the silicon-containing species. Furthermore, differences between double and triple bonds are smaller in the sulfides.

On the other hand, with respect to SENs, silicon compounds show unexpectedly larger differences between double and triple bonds than the analogous carbon-containing species. This demonstrates that the SENs for SiX_2 molecules are particularly small. The reason appears to be that the SiX_2 molecules show stronger ionic contributions to bonding, and this, in turn, is equivalent to weaker covalent bonding.

Conclusion

The molecule SiS_2 has been characterized by matrix IR investigation and by ab initio SCF calculations. With the help of these data, double and triple bonds in the systems C/O, C/S, Si/O, and Si/S are compared. The following trends can be deduced:

Bond parameters, which characterize a bond near the equilibrium position (bond distance and stretching force constant), exhibit significant differences only between double and triple bonds for the C/O system. The expected differences between the two multiple bonds are best described by bond energies, which characterize bonds at large distances. The SENs, which represent the covalent bonding contributions, are useful only to distinguish double and triple bonds, when ionic bonding is of comparable size in each. Therefore, in this respect, the more ionic silicon-containing molecules cannot be directly compared with the analogous carbon compounds.

Anyway, this discussion is an impressive example of the well-known fact that a bond cannot be described by a single parameter. A complete description can be given only by the whole potential function.

Acknowledgment. This work was supported by the Deutsche Forschungsgemeinschaft and in part by the Fonds der Chemischen Industrie. We thank M. Almond for corrections to the English text.

Registry No. SiS_2, 13759-10-9.

Systematic Effects of Crystal-Packing Forces: Biphenyl Fragments with H Atoms in All Four Ortho Positions

Carolyn Pratt Brock* and Robin P. Minton

Contribution from the Department of Chemistry, University of Kentucky, Lexington, Kentucky 40506-0055. *Received July 18, 1988*

Abstract: A comparison of observed and calculated distribution functions for the twist angle around the central C–C bond of biphenyl fragments with H atoms in all four ortho positions has been made. Reliable sets of coordinates for 101 such biphenyl fragments were retrieved from the Cambridge Structural Database. The calculated population distribution was derived from the Boltzmann inversion of an experimentally derived torsion potential for an isolated molecule; this potential has an energy minimum at a twist angle of 44° and small barriers at twist angles of 0° and 90°. Comparison of the observed and calculated distribution functions shows that nearly planar biphenyl fragments are found to occur much more often than expected. Nearly planar conformations, which lie ca. 6 kJ/mol above the minimum of the intramolecular potential energy surface, appear to be favored systematically in the solid state; contrary to the usual assumption of the structure correlation method, the effects of crystal packing on the molecular conformations of these fragments seem not to be completely random. Structures with twist angles below 12° were examined carefully; if possible, the atomic "thermal" parameters were analyzed in terms of the rigid-body model. Evidence of disorder was found for only one of these structures. Librational/torsional motion about the long axis of the biphenyl fragment is inversely correlated with twist angle: the more planar the molecule, the greater the motion. Increased motion raises the mean instantaneous distance between the ortho H atoms and thereby lowers the energy cost of a conformation that is planar on the average.

Comparisons of data from large numbers of crystal structures are commonly used to determine mean molecular geometries, deduce reaction pathways, and identify transition states.[1-3] These data are often retrieved from the Cambridge Structural Database[2,4] (hereafter, the CSD), a compendium of nearly 70 000 structures of molecular crystals; the general procedure is known as the structure-correlation method.[3] Underlying this method is the assumption that molecular structures concentrate in low-energy regions of conformational space in the solid state as they do in the gas phase.[3] But is this assumption always valid? Is it possible for the solid state to systematically favor a molecular conformation that does not correspond to an intramolecular energy minimum?

Conformations that do not correspond to an intramolecular energy minimum are observed from time to time in the solid state; their occurrence is attributed to crystal-packing effects. The structure-correlation method assumes that molecular deformations resulting from packing forces are small in terms of energy and that they are distributed randomly over the normal coordinates. The environment in any individual molecular crystal is almost always anisotropic, but if a structural fragment is observed in a large number of different environments, any directional effects are supposed to be averaged out. Effects of the generally greater density in the solid state, as compared with less condensed phases, are rarely considered. Taken together, these assumptions are

(1) Wilson, S. R.; Huffman, J. C. *J. Org. Chem.* **1980**, *45*, 560–566.
(2) Allen, F. H.; Kennard, O.; Taylor, R. *Acc. Chem. Res.* **1983**, *16*, 146–153.
(3) Bürgi, H.-B.; Dunitz, J. D. *Acc. Chem. Res.* **1983**, *16*, 153–161.
(4) Allen, F. H.; Bellard, S.; Brice, M. D.; Cartwright, B. A.; Doubleday, A.; Higgs, H.; Hummelink, T.; Hummelink-Peters, B. G.; Kennard, O.; Motherwell, W. D. S.; Rodgers, J. R.; Watson, D. G. *Acta Crystallogr.* **1979**, *B35*, 2331–2339.

0002-7863/89/1511-4586$01.50/0

equivalent to the expectation that a molecule will, on the average, crystallize in a conformation near the global minimum of its potential energy surface. This study examines that expectation with specific reference to biphenyls with H atoms in all four ortho positions, a class of molecules known to be especially susceptible to crystal-packing effects.[5]

Taking the structure-correlation method a step further, several authors have suggested that the observed distribution of structures, i.e., of sample points, might be fitted to a Boltzmann-like distribution (see, e.g., ref 3). This idea reflects the observation that molecular distortions are much more likely to be small than large. Several authors have used an exponential function to relate an observed distribution of sample points to an intramolecular potential energy surface. Kroon et al.[6] interpreted the histograms for O–H···O bonds in molecular crystals as Boltzmann distributions in order to derive force constants. They observed that "cases with a calculated energy of more than 1 kcal mol^{-1} above the optimum are very rare.". Brown[7] examined a series of compounds containing O–H···O hydrogen bonds and described the two-dimensional distribution with a function of the Boltzmann form. He noted that "the resulting map shows not the true energy but a description of the observed distribution expressed as an 'energy' and only certain features can be expected to correspond to the true potential energy". Taylor[8] used an empirical potential energy function and Monte Carlo techniques to calculate distribution functions for several angles describing O–H···O hydrogen bonds; he then compared these functions to observed distributions with considerable success. Murray-Rust[9] compared the distribution of sample points corresponding to the torsion angle about the C–O single bond in a series of 101 ethyl esters to the potential for rotation about the C–O bond in ethyl formate as determined by microwave spectroscopy, also with good success. Bye, Schwiezer, and Dunitz[10] interpreted the three-dimensional distribution of ring rotations for triphenylphosphine oxide fragments in terms of a Boltzmann function in order to estimate the barrier to stereoisomerization. They issued a warning, however, in characterizing the underlying assumption as "appealing though scarcely justifiable".

Dunitz et al. have pointed out a key problem with this analysis:[3,10] it is not clear what temperatures should be used in the expression $\exp(-E/RT)$. The structures comprising the sample populations have often been determined at a variety of temperatures, usually in the range 100–300 K. Furthermore, at any specific temperature, e.g. 300 K, the intermolecular forces in crystals containing hydrogen bonds or ionic interactions are substantially stronger than the forces in crystals held together by van der Waals interactions only. It is probably a reduced temperature that should be used in the exponential function, such as the ratio of the experimental to the Debye temperature, but these values are seldom available.

Very recently,[11] Lesyng, Jeffrey, and Maluszynska have used crystal structure data retrieved from the CSD to deduce a one-dimensional potential energy function for N–H···O=C and O–H···O=C hydrogen bonds. Their results support the structure-correlation principle but also demonstrate that the increased density in the solid state does affect the observed distribution of hydrogen bond lengths; they find the average crystal to be slightly compressive relative to the gas phase. In order to obtain satisfactory fits to the observed distributions using a Morse potential, they had to include three parameters describing the crystalline environment: an effective crystal-packing force, an average Debye temperature, and an average Gruneisen constant.

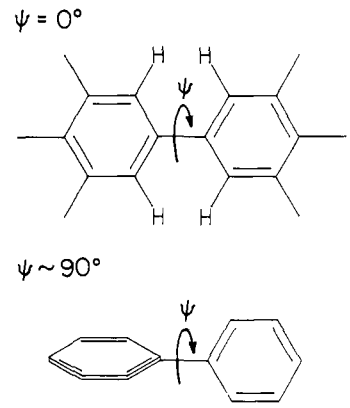

Figure 1. Angle ψ in an idealized biphenyl molecule.

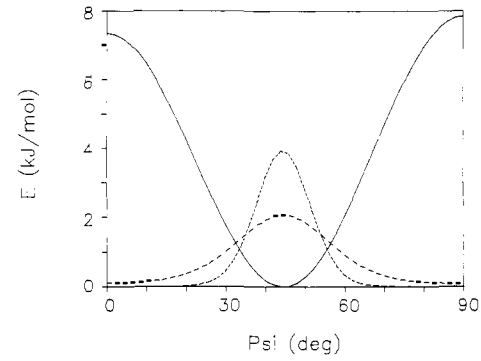

Figure 2. Average potential energy curve (solid line) for the torsional mode of ortho unsubstituted biphenyls determined by Bastiansen and Samdal.[14] The associated Boltzmann distributions calculated at 100 K (- - -) and 300 K (– –) are also shown.

Although the relationship between the intramolecular potential energy surface and the distribution of solid-state structures seems to be well established, our experiences studying biphenyl derivatives[12] led us to wonder whether biphenyl fragments might represent an important exception to the general rule that sample points cluster in low-energy regions of conformational space. Biphenyl itself is the classic example of a molecule affected by crystal-packing effects.[5] In the gas phase the average torsion angle (hereafter, ψ) about the central C–C bond is 44 (1)°,[5] while in the solid state ψ is close to 0°, at least at temperatures above 80 K.[13] The planar molecule is thought to be situated at a maximum of the intramolecular energy surface, about 6 kJ/mol above the minimum corresponding to the twisted molecule.[14] A number of simple biphenyl derivatives also have nearly planar structures in the solid state. A preliminary survey suggested that low ψ values are more common than expected.

Examination of biphenyl fragments without ortho substituents allows a fairly direct comparison of the observed and calculated distribution functions for ψ. This torsion angle is the only important intramolecular degree of freedom in the fragment (see Figure 1). The variation with ψ of the intramolecular potential energy has recently been determined by gas-phase electron diffraction, and substituent effects were found to be small.[14] The electron diffraction results are in basic agreement with quantum and molecular mechanics calculations.[14] Structures containing this fragment are plentiful in the CSD.

If any group of fragments is likely to be affected by systematic packing effects, it is the biphenyls without ortho substituents. The

(5) Almenningen, A.; Bastiansen, O.; Fernholt, L.; Cyvin, B. N.; Cyvin, S. J.; Samdal, S. *J. Mol. Struct.* **1985**, *128*, 59–76, and references therein.
(6) Kroon, J.; Kanters, J. A.; van Duijneveldt-van de Rijdt, J. G. C. M.; van Duijneveldt, F. B.; Vliegenthart, J. A. *J. Mol. Struct.* **1975**, *24*, 109–129.
(7) Brown, I. D. *Acta Crystallogr.* **1976**, *A32*, 24–31.
(8) Taylor, R. *J. Mol. Struct.* **1981**, *73*, 125–136.
(9) Murray-Rust, P. In *Molecular Structure and Biological Activity*; Griffin, J. F.; Duax, W. L., Eds.; Elsevier Science: New York, 1982; pp 117–133.
(10) Bye, E.; Schweizer, W. B.; Dunitz, J. D. *J. Am. Chem. Soc.* **1983**, *104*, 5893–5898.
(11) Lesyng, B.; Jeffrey, G. A.; Maluszynska, H. *Acta Crystallogr.* **1988**, *B44*, 193–198.
(12) (a) Brock, C. P.; Morelan, G. L. *J. Phys. Chem.* **1986**, *90*, 5631–5640. (b) Brock, C. P.; Haller, K. L. *Acta Crystallogr.* **1984**, *C40*, 1387–1390. (c) Brock, C. P. *Acta Crystallogr.* **1980**, *B36*, 968–971.
(13) (a) Charbonneau, G.-P.; Delugeard, Y. *Acta Crystallogr.* **1977**, *B33*, 1586–1588. (b) Charbonneau, G.-P.; Delugeard, Y. *Acta Crystallogr.* **1976**, *B32*, 1420–1423.
(14) Bastiansen, O.; Samdal, S. *J. Mol. Struct.* **1985**, *128*, 115–125.

energy cost of rotation about the central C–C bond is small, so that a small energy increment can correspond to a large change in the shape of the fragment. There is some evidence that the average value of ψ is at least 10° lower in solution than in the gas phase.[15] That result suggests that the torsion angle ψ may be especially sensitive to intermolecular interactions.

Methodology

Calculated Curves. An E vs ψ curve calculated from the composite energy function of Bastiansen and Samdal[14] is shown in Figure 2. The compounds on which this curve is based include biphenyl, biphenyl-d_{10}, and the biphenyl derivatives 4-fluoro-, 4,4′-difluoro-, 4-chloro-, 4,4′-dichloro-, 3,3′-dibromo-, 3,4′,5-tribromo-, and 3,3′,5,5′-tetrabromobiphenyl. Superimposed on the curve are the corresponding Boltzmann distributions calculated as $\exp(-E/RT)$ at temperatures of 300 and 100 K. These two curves have been normalized so that the areas they enclose are equal.

Database Search. Biphenyl fragments without ortho substituents were located in the Jan 1988 version of the Cambridge Structural Database; the search question is included with the supplementary material. The CSD program GEOM78 was used to compute the dihedral angle between the two rings (hereafter, D), the four torsion angles around the central C–C bond (hereafter, TOR_i, i = 1,4), and the length of the central C–C bond. The crystallographc agreement factor R and various error indicators for the structures were also tabulated. Eight additional structures were located for which coordinates have not yet been archived in the CSD.

An average conformation angle $\langle C\rangle = (\sum C_i)/4$, i = 1,4, and the associated estimated standard deviation $\sigma(C) = [(\sum C_i - \langle C\rangle)^2/3]^{1/2}$, i = 1,4, were derived from the four torsion angles TOR_i. Conformation angles C_1 and C_2 were chosen as the two torsion angles in the range $-\pi/2$ to $+\pi/2$. If the average of C_1 and C_2 was negative, all four TOR_i angles were multiplied by −1 (the equivalent of switching to the other enantiomer), and the calculation was restarted. The values of C_3 and C_4 were computed by adding 180° to each of the two remaining TOR_i values. This process guaranteed that all individual C_i values fall within, or very near the border of, the first quadrant. All average values $\langle C\rangle$ calculated in this way are in the range 0–90°.

All structures located were scrutinized carefully; in most cases the original papers were examined. Structures were excluded from the final tabulation if they failed any of the following tests:

1. $R < 0.15$. Structures with $0.10 < R < 0.15$ were investigated in detail. Some were kept; others were excluded.

2. $|\langle C\rangle - D| \leq 5°$. Values of $\langle C\rangle$ and D differ if the fragment is deformed in the region of the central C–C bond.

3. $\sigma(C) \leq 5°$. The values of the four conformation angles around the central C–C bond differ if the fragment is deformed in that region. Any hidden disorder of the ortho C atoms might also result in large values of $\sigma(C)$ or $|\langle C\rangle - D|$.

Structures were also eliminated for the following chemical reasons:

4. Fragment geometrically constrained. Penta-*m*-phenylene (PENMPH), hexa-*m*-phenylene (HEXMHP), [2.0.2.0]metacyclophane (DULVOV), and a biphenylo(4)phane (TTHPOP) were omitted on this basis.

5. Anionic fragment. Delocalization of the extra electron may favor planarity in anionic biphenylides. Structures containing organic cations (usually amines) or charged transition-metal complexes were retained.

6. Coordination of a metal atom or ion to the π system of the biphenyl fragment.

Finally, if the same phase was studied at more than one temperature, only the ψ value at one temperature was retained. In no case did the ψ value vary more than 1° with temperature.

Structures Containing Nearly Planar Fragments. Special attention was given to structures containing nearly planar biphenyl fragments; such structures have long been suspected (unnecessasrily, as it turns out) of being complicated by unrecognized disorder.[16] Structures in which the fragment is required to conform to inversion symmetry have been considered to be especially questionable. If the space group chosen imposes symmetry conditions on the biphenyl fragment, the paper was checked to see if the authors had considered the possibility of a lower symmetry group.[17]

The most sensitive test for hidden disorder is analysis of the anisotropic displacement parameters (hereafter, ADP's), the so-called "thermal" parameters.[18] If the ADP's make sense in terms of plausible molecular vibrations, then there is little likelihood that disorder has been overlooked. Disorder can be effectively ruled out if the mean-square amplitudes decrease approximately linearly with temperature and extrapolate to very small values at absolute zero. Thermal-motion analyses have been published for 7 of the 14 biphenyl fragments having $\langle C\rangle \leq 2.5°$ (BIPHEN,[13a,19] BOPSAA01,[12a] BOPSAA10,[12a] BUHSIG,[20] CIMCIK,[12b] FPhPhF[21]). All of the analyses give physically reasonable descriptions of the thermal motion. Five of the fragments were studied at multiple temperatures with the explicit goal of determining whether or not the structures are disordered. In none of the five was any evidence of disorder found.

Seven additional fragments, for a total of 21, have $\langle C\rangle \leq 12.5°$; refined ADP's are available for 8 of the 14 fragments not listed above. The ADP's for the ring atoms in these eight fragments were analyzed using Trueblood's program THMV10[18,22] to see if the ADP's make sense in terms of rigid-body motion. In two of the eight cases (BDTCNB10, BZTCNQ), the ADP's could not be fitted satisfactorily to a rigid-body model and are probably not of high quality. The remaining six (BPHLFE10, DOJWOO, MBZDCN, ZEGLAY, mBinap) gave adequate to good fits ($R < 0.20$).[23] In only one of the six cases was there any indication of hidden disorder. Of the total of 21 fragments having $\psi < 12.5°$, 12 undergo ordinary thermal motion, 8 cannot be judged according to this criterion, and 1 (ZEGLAY[24]) is probably complicated by hidden disorder (see below).

The structures of biphenyl (BIPHEN), *p*-terphenyl (TERPHE), and *p*-quaterphenyl (QUPHEN) require special consideration. At room temperature the three are isostructural and are required to conform to inversion symmetry. All undergo transitions at lower temperatures to phases in which the molecules are substantially twisted. Biphenyl, however, differs from the others. The apparent librational/torsional motion about its long molecular axis is not especially large at room temperature (see the Discussion),[13a] and the decrease in its motion as the temperature is lowered to 110 K is in approximate agreement with predictions based on a harmonic potential.[13b,19,25] The phase transitions, including a transition to an incommensurate phase, take place well below 80 K.[19] The value of $\psi = 0$ for BIPHEN was included in the final tabulation. In the longer polyphenyls, however, the corresonding motion of the central ring(s) is much larger at room temperature (260, 178 deg^2), and it decreases only slightly as the temperature is lowered.[26] Phase transitions take place at 191 K (TERPHE) and 243 K (QUPHEN),[26] and the structures of the ordered phases have been determined. For the high-temperature phases of TERPHE and QUPHEN, estimates of ψ were made based on the results of split-atom refinements (see Table I).[19,27] While the ψ values for these molecules are known somewhat less precisely than are the ψ values for other fragments, they are derived from studies done much more carefully than most.

Tabulation. The final tabulation includes 101 ψ values corresponding to 68 structures of 65 compounds. Three compounds have been studied in two phases each. A total of 10 of the structures have 2 or 3 biphenyl fragments in the same molecule or ion; 13 have 2, 3, or 4 molecules in the asymmetric unit. A total of 2 of these 23 structures, the low-temperature forms of *p*-terphenyl (TERPHE05) and *p*-quaterphenyl (QUPHEN01), have both. Values of ψ from the same structure are often, but by no means always, similar.

The ψ values listed in Table I and shown in the histograms (see below) are the average conformation angles, $\langle C\rangle$. These angles are a better

(15) Eaton, V. J.; Steele, D. *J. Chem. Soc., Faraday Trans. 2* **1973**, 1601–1608.

(16) The term disorder as used here implies population of two sets of atomic positions separated by an energy barrier that is at least comparable to kT.

(17) Imposed symmetry $\bar{1}$ (C_i) and $2/m$ (C_{2h}) require both $\langle C\rangle$ and D to be zero. A mirror plane may or may not require both $\langle C\rangle$ and D to be zero depending on its orientation, but in any event the angles are both very small.

(18) For a review of the interpretation of crystallographically determined anisotropic displacement parameters, see: Dunitz, J. D.; Schomaker, V.; Trueblood, K. N. *J. Phys. Chem.* **1988**, *92*, 856–867.

(19) Baudour, J. L.; Toupet, L.; Delugeard, Y.; Ghemid, S. *Acta Crystallogr.* **1986**, *C42*, 1211–1217.

(20) Pasimeni, L.; Guella, G.; Corvaja, C.; Clemente, D. A.; Vicentini, M. *Mol. Cryst. Liq. Cryst.* **1983**, *91*, 25–38.

(21) Lemee, M. H.; Toupet, L.; Delugeard, Y.; Messager, J. C.; Cailleau, H. *Acta Crystallogr.* **1987**, *B43*, 466–470.

(22) (a) Trueblood, K. N. *Acta Crystallogr.* **1978**, *34*, 950–954. (b) Schomaker, V.; Trueblood, K. N. *Acta Crystallogr.* **1984**, *40*, C339.

(23) Fits for ZEGLAY and mBinap are excellent ($R < 0.06$), the fit for DOJWOO is good ($R < 0.10$), and the fits for BPHLFE10 and MBZDCN are adequate ($R < 0.18$). Fits for BZTCNQ and BDTCNB10 are less good ($R < 0.25$), and the eigenvalues of the libration tensor are unreasonably small.

(24) Haase, W.; Paulus, H.; Müller, H. T. *Mol. Cryst. Liq. Cryst.* **1983**, *97*, 131–147.

(25) Busing, W. R. *Acta Crystallogr.* **1983**, *A39*, 340–347.

(26) Cailleau, H.; Baudour, J.-L.; Meinnel, J.; Dworkin, A.; Moussa, F.; Zeyen, C. M. E. *Faraday Discuss. Chem. Soc.* **1980**, *69*, 7–18.

(27) Baudour, J.-L.; Cailleau, H.; Yelon, W. B. *Acta Crystallogr.* **1977**, *B33*, 1773–1780.

measure of the torsion around the central C–C bond than are the dihedral angles, D, especially if the fragment is bowed or bent. Of the 101 determinations of ψ, 71% have $\sigma(C) \leq 1°$ and 82% have $\sigma(C) \leq 2°$. The estimated standard deviation of the mean, $\sigma(\langle C \rangle)$ is smaller still by the factor, $4^{1/2} = 2$. In no case is the difference between $\langle C \rangle$ and D greater than 2°; in most cases it is much less. We conclude from the above that most ψ, i.e. $\langle C \rangle$, values are known to within 2° or better.

Although most ψ values are well determined, a few of the very small values may be in error by as much as 10–15°. As a cautionary example, consider *p*-terphenyl (TERPHE). Room-temperature data for this compound were originally refined with a planar molecule to an R factor below 0.10,[28] but later work[19,27] showed a double-well model ($\psi \sim 13°$) to be more appropriate. Our analysis of the published ADP's of the biphenyl fragment in 4′-cyano-4-(4-*N*-pentylcyclohexyl)biphenyl (ZEGLAY)[24] reveals very large apparent librational motion about the C4–C4′ fragment axis. The value of almost 200 deg^2 is comparable to that seen for the central ring of "planar" *p*-quaterphenyl and so suggests that disorder has been overlooked, even though the final crystallographic agreement factor was below 0.07. On the other hand, the motion in 12 other nearly planar fragments is reasonable (see above, and also the Discussion). The maximum number of structures affected by this kind of error is nine, but the actual number is probably a great deal lower.

The REFCODEs, compound names, and ψ values for structures both included in and excluded from the final tabulation are given in Table I; information about any imposed symmetry and the temperature of the determination is also shown. All structures located by the search and having archived coordinates are accounted for. Full literature references are included in the supplementary material. Also given there are the specific reasons for discarding the 16 structures corresponding to 29 ψ values in the second part of Table I.

Distributions. The one-dimensional energy surface for rotation about the central C–C bond of an idealized biphenyl molecule has a period of π. The curve has inversion points at $\psi = 0$ and $\psi = \pi/2$ so that the unique part may be taken as $0 \leq \psi \leq \pi/2$. If there are no ortho substituents, if there are no important distortions from idealized geometry, and if there are no significant effects from any meta or para substituents, then the E vs ψ curve for biphenyl fragments is the same as for the unsubstituted biphenyl molecule.

As a result of the procedure for determining $\langle C \rangle$ (see above), all observed values of ψ lie in the range $0 \leq \psi \leq \pi/2$. It is important to remember, however, that, for every observed value $0 < \psi < 90°$, there is a corresponding value $-90° < \psi < 0$ for the other enantiomer and that this second value has not been included in the tabulation. The two enantiomers may occur in the same crystal or in pairs of chiral crystals grown from a racemic mixture, but in either case only one of the two sets of coordinates is included in a CSD entry. If the structure has been determined more than once, the several sets of coordinates may or may not correspond to the same enantiomer, but in any event only one of them would have been included in our tabultion.

When constructing a histogrammic representation of the observed distribution, both the sizes of the bins and the locations of the bin boundaries relative to the symmetry elements must be chosen. Histograms were constructed with bin sizes of 2, 5, and 9°. Although the 2° bin size is appropriate for the precision of the ψ values, there are not very many values per bin. The 5° bin size is better in this regard. The 9° bins are better yet, but resolution is lost.

Bins may be centered either at $90m/n$ degrees ($0 \leq m \leq n$) or at $45\ (2m + 1)/n$ degrees ($0 \leq m < n$). In the latter case the bin *boundaries* are located at $\psi = 0$ and 90°, while in the former case bins are *centered* on those stationary points. A choice must also be made as to how to count ψ values that fall exactly on a bin boundary. Consider 5° bins with boundaries at the inversion points. If the bin ranges are 0.00–4.99, 5.00–9.99, ..., 175.00–179.99°, all values in a bin are given full weight. If, however, the ranges are 0.00–5.00, 5.00–10.00, ..., 175.00–180.00°, then the values on the boundaries are counted in two bins and must be given half-weight. If only the unique part of the histogram is to be displayed and if the sum of the bar heights should equal the number of entries in Table I, then the first bin must contain values $0 \leq \psi < 90m/n$ degrees ($0 \leq m \leq n$). The disadvantage of this choice is that the histogram is not symmetric about $\psi = 0$ and that the representation may seem to overemphasize the observations in the first bin. A second possibility would be to count, with half-weight, the 11 values at $\psi = 0.00°$, all of which are constrained by symmetry, in the bins on both sides of the origin. In that case the bins on each side of the origin would contain the same number of observations, but the total number of observations displayed in the unique part of the distribution would be less than the number of entries of Table I.

(28) Rietveld, H. M.; Maslen, E. N.; Clews, C. J. B. *Acta Crystallogr.* **1970**, *B26*, 693–706.

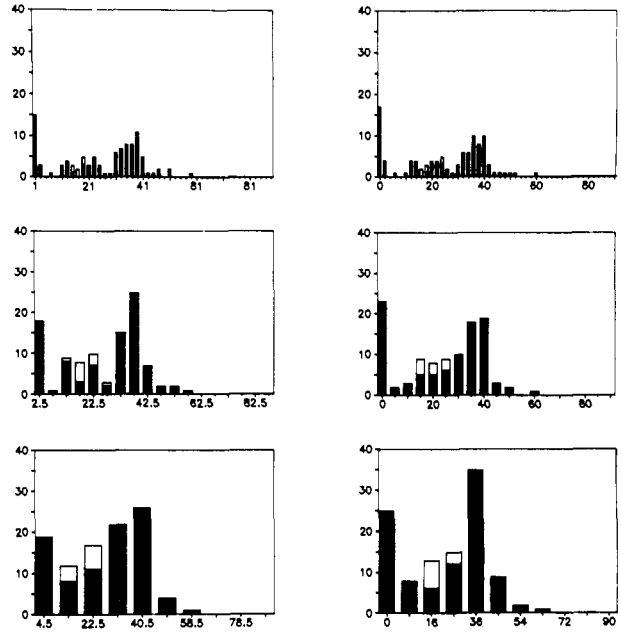

Figure 3. Distributions of sample points for bin sizes of 2, 5, and 9°. Two choices for the bin boundaries are shown in each case: (a) first bin starts at 0° (left column of figure); (b) first bin is centered at 0° (right column of figure). The unfilled areas of the bars ($14 < \psi < 27°$) represent the 10 ψ values from the low-temperature forms of *p*-terphenyl and *p*-quaterphenyl (see text).

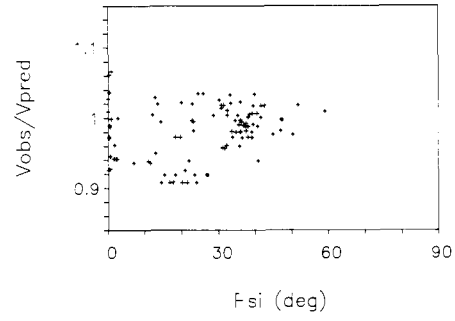

Figure 4. Plot of V_{obs}/V_{pred} vs ψ (see text).

If the choice is made to center the bins on the inversion points, then the first bin must include negative ψ values if all the bins are to be the same width. The resulting histogrammic representation has the correct symmetry, but more than the unique part of it must be displayed. The 11 values at $\psi = 0$ are effectively given half-weight relative to the twisted molecules in the same bin, which are counted at both $+\psi$ and $-\psi$.

Figure 3 displays histograms constructed from the 101 ψ values for bin sizes of 2, 5, and 9°. Two choices of bin boundaries are illustrated. In the first column of Figure 3, the first 5° bin covers the range 0.00–4.99°, and all observations are given equal weight. In the second column of Figure 3, the first 5° bin covers the range −2.50 to +2.50, and observations at $\psi = 0.00°$ are effectively given half-weight. We prefer the second choice because it better reflects the symmetry of the problem but admit that this choice, like all the others discussed above, has drawbacks. What is more interesting, however, is how important the choices of bin size and boundaries are to the overall appearance of the histogrammic representation of the distribution.

Predicted Volumes. Unit-cell volumes for each structure were estimated from the unit-cell contents using Stalick's set of approximate atomic volumes determined for molecular crystals (See Table II).[29] The ratio V_{obs}/V_{pred} is plotted against ψ in Figure 4.

Results

The observed (Figure 3) and Boltzmann (Figure 2) distributions differ in important ways. The former is much more asymmetric

(29) (a) Stalick, J. K. *Abstracts of Papers*, Winter Meeting of the American Crystallographic Association, Columbia, MO, March 1983; American Crystallographic Association: New York, 1983; Abstract PA9. (b) Stalick, J. K., personal communication, 1986.

Table I. List of Structures Retrieved from the Jan 1988 Version of the Cambridge Structural Database

REFCODE	sym[a]	temp,[b] K	ψ, deg	name (as it appears in the CSD)[e]
			I. Structures Included in the Final Tabulation	
ABRBPH			38.1	4-acetyl-3′-bromobiphenyl
ACLBPH			20.8	4,4′-diamino-3,3′-dichlorobiphenyl
ACNBPC	222		33.2	diammine-nickel(II) tetracyanonickelate(II) bis(biphenyl)
ACTHBZ		138	31.8	*N*,*N*′-diacetyl-3-methylthiobenzidine
BAZLOD			36.5, 39.2	bis(4-biphenylyl)-sulfur-diimide
BDEAUCU10			13.4, 22.8	μ-benzidine-bis(2,2′,2″-triaminotriethylamine)-di-copper(II) nitrate
BDTCNB10	*m*		0.0	benzidine-7,7,8,8-tetracyanoquinodimethane complex, benzene solvate
BDTNBB			19.9	benzidine-*S*-trinitrobenzene complex, benzene solvate
BIPHEN03	*i*	110	0.0	biphenyl
BIPHSB10			38.5	biphenyl bis(antimony trichloride)
BNZTNB	2		12.8	benzidine-*S*-trinitrobenzene complex
BODJOT	*i*		0.0	18-crown-6, 4,4′-biphenyldiol, dihydrate
BOPSAA01			2.1, 2.5	4-hydroxybiphenyl (orthorhombic form)
BOPSAA10			1.6	4-hydroxybiphenyl (monoclinic form)
BOPSEE10			28.7, 32.4, 35.3	4-biphenyl carboxylic acid
BPHAMP10			14.4, 23.2, 36.3	tri(*p*-biphenylyl)aminium perchlorate
BPHFPA[c]			35.9	4-methylbiphenyl, perfluorobiphenyl complex
BPHFPB[c]			37.5	4-bromobiphenyl, perfluorobiphenyl complex
BPHLFE10			6.9, 11.5	4-biphenylferrocene
BPPFBP	2		36.1	biphenyl, perfluorobiphenyl complex
BRBIPH		152	18.3, 19.7	4-bromobiphenyl
BRCYBP			41.6, 42.5	4-bromo-4′-cyanobiphenyl
BTOLYL			35.6, 39.5	*p*,*p*′-bitolyl
BUCTUO			12.0	1,2,4,5-dianhydro-3-*O*-(4-phenylbenzoyl)-xylitol
BUHSIG	*i*		0.0	biphenyl 1,2,4,5-tetracyanobenzene
BZOBPH			0.6	4,4′-dibenzoylbiphenyl
BZTCNQ	2/*m*		0.0	benzidine-7,7,8,8-tetracyanoquinodimethane complex
CAPZEY			24.4, 25.9	(3,3′-dimethoxy-4,4′-bis(3-methyltriazene-3-oxide) biphenyl)-di-copper(II)
CELDOM			46.9	4-biphenylyl phenyl thioketone
CEYTEF			30.8	3-chlorobiphenyl-4-carbonitrile
CIMCIK			0.4, 37.4, 36.9, 37.2	tris(4,4′-dinitrobiphenyl) 4-hydroxybiphenyl
CINGEL			13.3, 39.6	1,1,6,6-tetraphenyl-1,6-bis(biphenylyl)-hexa-2,4-diyne, *p*-xylene clathrate
COPRAA			59.0	[(4-phenyl-benzoyl)-(triphenylphosphine)-methylene]-*o*-tolyl-iodonium tetrafluoroborate
COSHUN			36.0, 47.2	1,3,5-tris(4-biphenylyl)benzene, benzene solvate
COSJAV			30.8, 31.4, 51.7	1,3,5-tris(4-(1,2-dicarba-*closo*-dodecaboran(12)-1-yl-methyl)phenyl)-benzene, chloroform solvate
DABMIC			33.2	2-*p*-biphenylisopropyloxycarbonyl-L-isoleucine
DADMBP			40.9	4,4′-diamino-3,3′-dimethylbiphenyl
DAFHEX			37.6	4-acetyl-3′-chlorobiphenyl
DBRBIP			38.1, 40.7	4,4′-dibromobiphenyl
DCLBIQ10			38.1, 41.5	4,4′-dichlorobiphenyl
DOJWOO			0.3	4′-*n*-pentyloxy-4-biphenylcarbonitrile
DPMBSB10			39.8	biphenyl-4,4′-bis(diphenylmethylium) hexachloroantimonate
DUMROS			39.5	4′-*n*-butyl-4-cyanobiphenyl
FABHEV			33.6	2-bromo-4′-phenylacetophenone
FABZAJ[c]			23.2	4-hydroxybiphenyl, acetone solvate
FAMHEG			50.3	2,6-bis(hydroxymethyl)-4-phenylphenol
FAVTAX			33.8	4,4′-dichloro-3,3′,5,5′-tetrafluorobiphenyl
FAZGES[c]			39.2, 40.5	4-bromo-4′-fluorobiphenyl
FLBIPC01			35.7	3′-fluorobiphenyl-4-carboxylic acid
IBPBAC01			34.5	isobutyl-4-(phenylbenzylideneamino)cinnamate
IBPCHA			32.3	3′-iodobiphenyl-4-carboxylic acid
MBZDCN	*i*		0.0	*N*,*N*,*N*′,*N*′-tetramethylbenzidine, chloranil complex
MPHOYZ			44.9	(3*S*,5*R*)-3-methyl-5-(4′-biphenylyl)-2,3,5,6-tetrahydro-1,4-oxazin-2-one
NBPHEN			32.4	*p*-nitrobiphenyl
NIOBPH	*i*		0.0	4,4′-dihydroxy-3,3′,5,5′-tetranitrobiphenyl
PTBPHN10	2/*m*		0.0	4,4′-bis(chloro-bis(triethylphosphine)-platinum-amino)-biphenyl hexafluorophosphate
QUPHEN	*i*		~22[d], ~11[d]	*p*-quaterphenyl (room-temperature form)
QUPHEN01		110	14.4, 16.8, 17.5, 20.0, 21.3, 24.0	*p*-quaterphenyl (low-temperature form)
TERPHE05		113	15.2, 18.2, 23.4, 26.8	*p*-terphenyl (low-temperature form)
TERPHE07			~13[d]	*p*-terphenyl (room-temperature form)
TMBCAN			31.2	*N*,*N*,*N*′,*N*′-tetramethylbenzidine-chloranil complex
TPHBEN01			34.8, 35.9, 39.2	1,3,5-triphenylbenzene
ZEGLAY			2.6	4′-cyano-4-(4-*n*-pentylcyclohexyl)-biphenyl
ZEGLIG			22.8	4-(4-*N*-propylcyclohexyl)-biphenyl
FPhPhF[c]	*i*		0.0	4,4′-difluorobiphenyl
mBinap[c]	*i*		0.0	*m*-binaphthyl
NCBphF[c]			30.2	4-cyano-4′-fluorobiphenyl
SPhPhS[c]	*i*		0.0	4,4′-biphenyldithiol
			II. Structures Omitted from the Final Tabulation	
BABKUK		130	3, 5, 7, 30	disodium diterphenylide terphenyl, 1,2–dimethoxyethane solvate
BDTCQC10	2/*m*		0	benzidine-7,7,8,8-tetracyanoquinodimethane complex, dichloromethane solvate
BENZID	*i*	110	0	benzidine dihydrochloride

Table I (Continued)

REFCODE	sym[a]	temp,[b] K	ψ, deg	name (as it appears in the CSD)[e]
BPTGLK	*i*	120	0	potassium biphenyl bis(2,5,8,11,14-pentaoxa-pentadecane)
CUCCIM			29, 30	4-(4′-bromophenyl)-phenacyl-(+)-2,3-decadienoate
DAMDAW			19	1-(η-6-biphenyl)-2,3-diethyl-1-ferra-2,3-dicarbaheptaborane
DNTDPH			33	4,4′-dinitrodiphenyl
DOHDPH10	*i*		0	4,4′-dihydroxydiphenyl
DULVOV			45, 51	[2.0.2.0]metacyclophane
HEXMHP01			28, 34, 36	hexa-*m*-phenylene
NABPEX			5	sodium biphenylide, 1,2-bis(2-methoxy)ethane solvate
PENMPH01			17, 25, 34, 38, 39	penta-*m*-phenylene (monoclinic form)
PRTPCX			2, 12	di-*n*-propyl-*p*-terphenyl-4,4-dicarboxylate
RBBIPH			9	rubidium biphenyl, di(2-(2″-methoxy-2′-ethoxy)ethyl)ether solvate
TAZHMP			2	4,4‴,6,6‴-tetra-aza-hexa-*m*-phenylene
TTHPOP			12, 15	2,17,32,35-tetrathia(3.3.3.3)(3,5′,5,3′)biphenylo(4)phane

[a] Crystallographically imposed symmetry that limits possible values of ψ. [b] Temperature if other than room temperature. [c] See supplementary material for additional information about the source of the coordinates. [d] Estimate derived from refinement of double-well (or, split-atom) model. [e] Compound names in the CSD contain no lower case, Greek, or italicized letters, and often contain extra hyphens.

Table II. Atomic Volumes (Å^3) Used To Predict Molecular Volumes[29]

H	5.4	Na	18	K	31
B	13.0	P	30	Fe	29
C	13.9	S	26	Ni	26.5
N	11.0	Cl	25	Cu	24
O	10.0	Br	30.5	Sb	46
F	11.5	I	44	Pt	42

and complex than the latter. The observed distribution has at least two, and maybe three, maxima, while the calculated function has only one.

The observed distribution, at least as represented by the histograms with the 2 and 5° bins, appears to have maxima centered at about ψ = 0, 18, and 37°; the ratios of the numbers of corresponding sample points are approximately 2:3:6. The largest maximum corresponds to the average conformation predicted and observed for the gaseous state (ψ = 44°),[14] although it is centered at a slightly lower value of ψ (37°). At higher ψ values, the distribution appears to drop off from the maximum more or less exponentially. There are no structures with ψ > 60° and very few with ψ > 50°.

The maximum in the distribution at ψ = 0° is sharper than the maximum at 37° but corresponds to only about $^1/_3$ as many biphenyl fragments. The greater height of the ψ = 0° maximum when a bin is centered at 0° (see, e.g., Figure 3b) is a result of the clustering of values very near ψ = 0°. There are 18 ψ values in the range 0–2.6°; the next smallest value is 6.9°. Of these 18 values, 7 correspond to fragments with no imposed crystallographic symmetry. Of the remaining 11 fragments, 8 are required to conform to inversion symmetry, 1 to mirror symmetry, and 2 to $2/m$ symmetry. A few, but certainly not many, of the ψ values in this range may be underestimated (see above).

Finally, there may be a broad maximum centered at about ψ = 18°. This feature must be viewed with some skepticism, however, because 10 of the 30 observations come from the low-temperature phases of *p*-terphenyl (two ψ values in each of two independent molecules) and *p*-quaterphenyl (three ψ values in each of two independent molecules). If these 10 values are removed from the distribution (see Figure 3), the intermediate maximum becomes much less prominent. It even disappears for some choices of bin size and boundaries.

Discussion

The data collected indicate that crystal-packing effects systematically stabilize biphenyl fragments with small twist angles ψ. Fragments with ψ < 20° are very much more common than would be predicted from a Boltzmann inversion of the potential energy curve of Bastiansen and Samdal.[14] The basic assumption of the structure-correlation method appears to be invalid for these molecules. The uncertainty about a few of the very small ψ values does not affect this conclusion.

There is little chance that the intramolecular potential energy curve determined by Bastiansen and Samdal[14] is seriously in error.

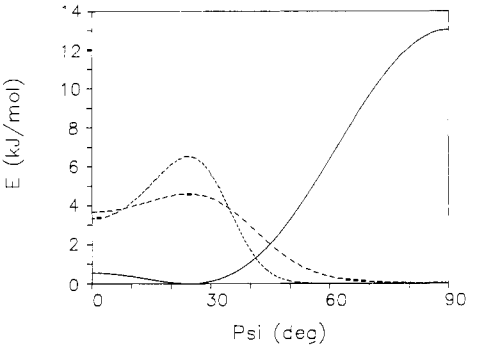

Figure 5. Potential energy curve and associated Boltzmann distributions at 100 K (---) and 300 K (--) for a hypothetical case in which $E(0) \ll E(\pi/2)$. E has the functional form $E(\psi) = (E_2/2)(1 - \cos 2\psi) + (E_4/2)(1 - \cos 4\psi)$.

It is in basic agreement with the many spectroscopic studies and quantum mechanical and molecular mechanics calculations and is rather insensitive to the presence of substituents in the meta and para positions.[14] No study of any type suggests that the energy curve has multiple minima. Estimates of the relative heights of the barriers at ψ = 0 and ψ = 90° vary between theoretical studies and with substituents, but most are within several kilojoules per mole of the values given by Bastiansen and Samdal for the composite curve.[14] Even if the barrier at ψ = 0° were negligible and the barrier at ψ = 90° relatively large, the resulting Boltzmann curve would not match the observed distribution. In the extreme (and hypothetical) case shown in Figure 5, the population distribution is expected to have a single, broad maximum centered at about ψ = 25°. There is no way to explain the two-humped, or perhaps three-humped, distribution that is observed (Figure 3) as a Boltzmann distribution without requiring that the energy curve for the molecular torsion have multiple minima in the range $0 \leq \psi \leq 45°$.

There seem to be only three explanations for the observed distribution. Perhaps the structures found in the CSD do not accurately represent the distribution that would be obtained if many more structures were available. Perhaps substituents in the meta or para positions have a much greater effect than expected on the preferred conformation. Finally, it is possible that the solid state systematically favors nearly planar biphenyl fragments because they pack better. The last explanation seems to be the most likely.

There is little doubt that the classic herringbone arrangement of nearly planar molecules that is found in the structure of unsubstituted biphenyl is very favorable. A sign of the special stability of this arrangement is the variety of substituents that can be added without disrupting the overall pattern. Crystals of *p*-terphenyl (TERPHE), *p*-quaterphenyl (QUPHEN), 4,4′-difluorobiphenyl (FPhPhF), 4,4′-hydroxybiphenyl (DOHDPH), and *m*-binaphthyl (mBinap) are all isostructural with biphenyl itself. The structures of 4-bromobiphenyl and of the two forms of 4-

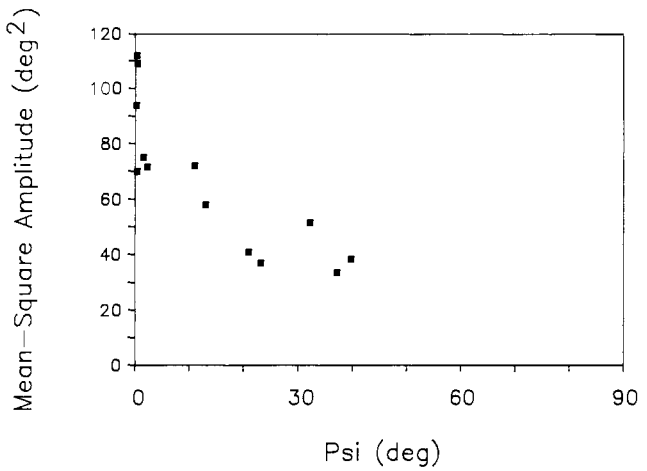

Figure 6. Plot of the mean-square amplitude of the librational motion associated with the long molecular axis (C4–C4′) of the biphenyl fragment vs ψ. Values are plotted for biphenyl in two environments (BIPHEN03,[13a] BUHSIG[20]), for 4-hydroxybiphenyl in four environments (BOBSAA01,[12a] BOPSAA10,[12a] CIMCIK,[12b] FABZAJ[12a]), for 4-biphenylcarboxylic acid (BOPSEE10),[31] for 4,4′-difluorobiphenyl (FPhPhF[21]), for 4,4′-dichlorobiphenyl (DCLBIQ10[32]), for 4,4′-dinitrobiphenyl (CIMCIK[12b]), for *p*-quaterphenyl (QUPHEN[33]), and for *p*-terphenyl in two phases (TERPHE05,[34] TERPHE07[19,27]). If separate values were determined for the two phenyl rings, or for several molecules in very similar environments, they have been averaged. The mean-square amplitudes determined for FABZAJ at 134 K (ψ = 23°) and TERPHE05 at 113 K ($\langle\psi\rangle$ = 21°) have been multiplied by the factor $295/T$.[35] Estimated standard deviations for individual points may reach 10% of the values plotted.

hydroxybiphenyl are very similar. The herringbone motif can also be spotted in some of the more complicated structures, such as those of 4-biphenylferrocene (BPHLFE10) and 4′-cyano-4-(4-*N*-pentylcyclohexyl)biphenyl (ZEGLAY). In none of these cases is ψ greater than 25°. It may be that the existence of this very favorable packing arrangement accounts for the observed distribution of ψ values.

Favorable packing arrangements are often associated with increased density, so it seemed possible that ψ values might be correlated with packing efficiency. The apparently lower average value of ψ for biphenyl in the liquid, as opposed to the less dense gaseous phase,[15] supports this idea. Finding a good measure of packing efficiency, however, proved difficult; direct comparisons of densities of compounds containing different atom types are not meaningful. We thought comparisons of the ratios of observed unit-cell volumes to unit-cell volumes calculated from a standard set of atomic volumes might reveal a trend, but they did not (see Figure 4).

The absence of a correlation between V_{obsd}/V_{pred} and ψ may result from the combination of two competing effects. More planar fragments may pack more densely, but they also seem to be associated with larger thermal motion. Busing[25] noted that the average structure of biphenyl can be planar at high temperatures because the mean *instantaneous* distance between the ortho H atoms is much larger than the distance between their mean atomic positions. Brock, Schweizer, and Dunitz[30] made a similar argument in suggesting that proximity to a partial maximum of the intramolecular potential energy surface can be correlated with the amplitude of motion along the corresponding internal coordinate, even in the solid state where mixing with lattice modes may be substantial. If that suggestion is correct, nearly planar biphenyl fragments can be expected to undergo large-amplitude torsional motion.

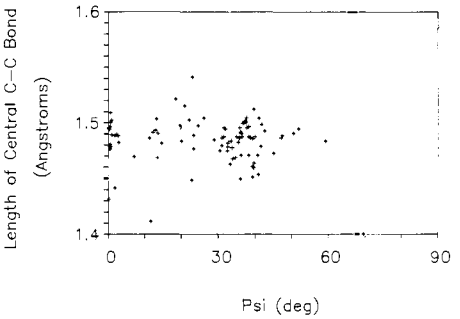

Figure 7. Plot of the length of the central C–C bond of the biphenyl fragment vs ψ.

Reliable, crystallographic determined descriptions of molecular motion are relatively rare but have been published for 12 of the structures in Table I. All of the molecules are simple biphenyl derivatives; in all cases substituents are located in the para positions. Consequently, the 2-fold rotation symmetry about the long molecular axis is retained, and the moments of inertia around this direction are the same for all the biphenyl fragments. Unfortunately, this symmetry precludes separation of the effects of the internal torsional motion, which is expected to depend on ψ, from the overall molecular libration about the long molecular axis, which should depend only on intermolecular interactions. The torsion and libration differ only in the relative phases of the motions of the two phenyl rings and are indistinguishable crystallographically. Nevertheless, even the combined motion shows the anticipated correlation: the smaller the value of ψ, the greater the amplitude of the motion (see Figure 6). The data on which this figure is based are given in the supplementary material.

Figure 6 suggests that the average mean-square libration at 300 K around the long molecular axis is about 90 deg^2 when ψ = 0° and about 40 deg^2 when ψ = 40°. It is reasonable to assume that molecular libration accounts for 50–75% of the motion for ψ = 40°, that is, 20–30 deg^2. If the librations of the twisted and planar conformations are similar, then the mean-square torsional amplitude in the planar molecules would be about 60–70 deg^2. If the root-mean-square torsional displacement of each ring is about 8°, the mean instantaneous torsion angle is well above zero, and most of the time the fragment is substantially twisted. The histograms would undoubtedly agree better with the population distribution derived from the potential energy function if they could be corrected for the effects of torsional motion. Such a correction, however, is well beyond the scope of the structure-correlation method as it is normally applied. Such a correction also requires information about the variation of the thermal motion with the structural parameter(s) of interest, but that information is seldom available.

An estimate of the effect of the torsional motion on the mean instantaneous distance between the ortho H atoms can be made using the method outlined by Busing.[25] Consider, for example, the three crystal forms of 4-hydroxybiphenyl, in each of which the experimentally determined C–H distances average 0.98 Å. In the two unsolvated modifications of 4-hydroxybiphenyl[12a] the ψ values are nearly zero and the mean H···H distance across the central C–C bond is 2.03 Å at ca. 80 K. Allowance for a torsional amplitude of 65 deg^2 lengthens this distance by 0.08 Å. The resulting value of 2.11 Å can be compared to the value of 2.13 Å determined at 133 K for the acetone solvate of 4-hydroxybiphenyl[12a] in which ψ = 23°. The correction for a molecule with

(30) Brock, C. P.; Schweizer, W. B.; Dunitz, J. D. *J. Am. Chem. Soc.* **1985**, *107*, 6964–6970.
(31) Brock, C. P.; Blackburn, J. R.; Haller, K. L. *Acta Crystallogr.* **1984**, *B40*, 493–498.
(32) Brock, C. P.; Kuo, M.-S.; Levy, H. A. *Acta Crystallogr.* **1978**, *B34*, 981–985.
(33) Delugeard, Y.; Desuche, J.; Baudour, J.-L. *Acta Crystallogr.* **1976**, *B32*, 702–705.
(34) Baudour, J.-L.; Delugeard, Y.; Cailleau, H. *Acta Crystallogr.* **1976**, *B32*, 150–154.
(35) For a harmonic crystal well above the Debye temperature, $\langle u^2\rangle = cT$, where $\langle u^2\rangle$ is a mean-square displacement and c is a constant. Essentially all crystals are anharmonic and expand as the temperature rises; the constant c then itself increases with T. Consequently, the extrapolated values shown in Figure 6 for FABZAJ and TERPHO05 may be too small by 15% or more.[36]
(36) Brock, C. P.; Dunitz, J. D. *Acta Crystallogr.* **1982**, *B38*, 2218–2228.

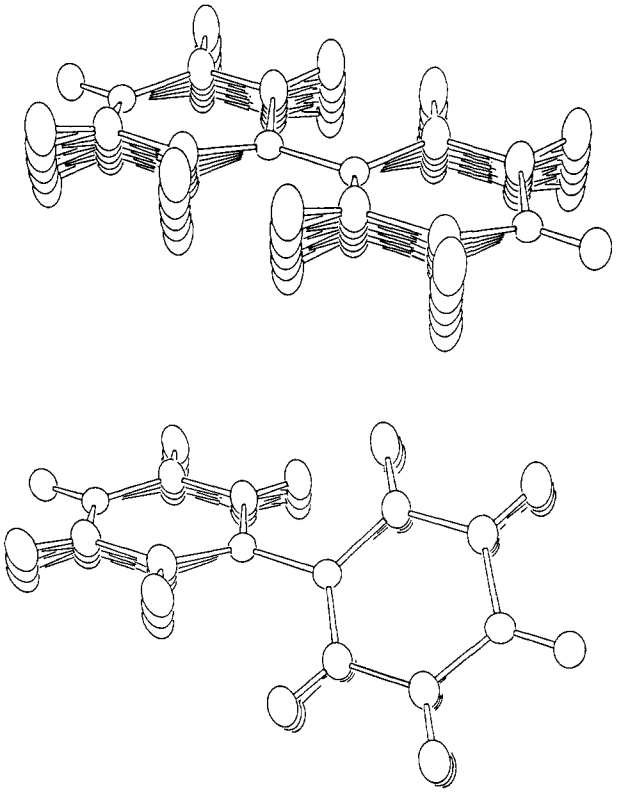

Figure 8. Planar and twisted (ψ = 45°) biphenyl molecules drawn to illustrate the greater molecular motion in the more planar conformation. The root-mean-square libration/torsion about the long molecular axis is ca. 10° in the planar conformation but only ca. 5° in the twisted conformation. The motion is simulated by the superposition of drawings that are separated by rotations of 5°.

ψ = 20° and a mean-square torsional amplitude of 25 deg^2 is smaller, only about 0.03 Å.

A side benefit of this study is the possibility of determining whether or not the length of the central C–C bond is correlated with ψ. Figure 7 shows that it is not. The average bond length of 1.484 Å for n = 91[37] molecules is in good agreement with the published value of 1.487 Å determined for a smaller sample of n = 30 values.[38] Stricter criteria were applied in choosing the more limited sample (e.g., $R \leq 0.07$), so that its sample standard deviation is smaller (0.007 Å vs 0.019 Å). The estimated standard deviations of the two mean values, however, are smaller by factors of $n^{1/2}$ and are both ≤0.002 Å.

(37) There are 10 fewer C–C distances than there are ψ values because the inter-ring C–C distance was fixed in the refinements of the low-temperature forms of *p*-terphenyl (four fragments) and *p*-quaterphenyl (six fragments).

Summary

Although ortho unsubstituted biphenyls are an important exception to the structure-correlation principle, they also seem to be unusual exception. Their characteristics may help define the limits of the method. First, the shape of a biphenyl is easily changed and is thus especially responsive to its environment. Fragments for which large-amplitude motions are associated with small energy changes are the most likely to give distributions that differ from the distribution derived from the intramolecular potential. Second, more planar conformations of biphenyls appear to pack better. Perhaps the solid state favors fragment planarity generally. It is also possible that the increased symmetry of planar, as compared with twisted, biphenyl fragments is a factor.

This study also demonstrates the importance of considering the dynamic properties of molecules in crystals (see also references 18 and 25). The relatively common occurrence of biphenyls with small torsion angles is easier to understand when the molecular motion is considered. The torsional amplitude and the value of ψ are almost certainly inversely correlated (see Figure 8). Increased motion raises the mean instantaneous distance between the ortho H atoms and thereby lowers the energy cost of a conformation that is planar on the average.

Addendum. Since this manuscript was submitted for publication, Bürgi and Dunitz have published[39] a critique of several studies in which observed population distributions were fitted by functions of the Boltzmann form. They conclude that the assumptions underlying the derivation of quantitative energy relationships from the distributions of fragment geometries observed in a variety of crystal environments is unwarranted.

Acknowledgment is made to the donors of the Petroleum Research Fund, administered by the American Chemical Society, for support of this research. We are also grateful to several colleagues and a reviewer who commented extensively on the original manuscript.

Supplementary Material Available: Tables giving the search question (Table S-I), giving bibliographic citations for all structures retrieved with coordinates from the Jan 1988 version of the Cambridge Structural Database (Table S-II), and giving more details about the information displayed in Figure 6 (Table S-III) (13 pages). Ordering information is given on any current masthead page.

(38) Allen, F. H.; Kennard, O.; Watson, D. G.; Brammer, L.; Orpen, A. G.; Taylor, R. *J. Chem. Soc., Perkin Trans. 2* **1987**, S1–S19.
(39) Bürgi, H.-B.; Dunitz, J. D. *Acta Crystallogr.* **1988**, *B44*, 445–448.